INSTITUTE OF PHYSICS PUBLISHING JOURNAL OF PHYSICS B: ATOMIC, MOLECULAR AND OPTICAL PHYSICS

J. Phys. B: At. Mol. Opt. Phys. **35** (2002) L537–L542 PII: S0953-4075(02)53098-4

LETTER TO THE EDITOR

An interplay between momentum distortion and electronic correlation in symmetric (e, 3−1e) reactions

K A Kouzakov[1] **and Yu V Popov**[2]

[1] Max-Planck-Institut für Mikrostrukturphysik, Weinberg 2, D-06120 Halle, Germany
[2] Nuclear Physics Institute, Moscow State University, Moscow 119899, Russia

E-mail: kouzakov@mpi-halle.de

Received 27 August 2002, in final form 11 November 2002
Published 27 November 2002
Online at stacks.iop.org/JPhysB/35/L537

Abstract

A theory is proposed for the treatment of the effects of distortion in electron-impact double ionization of atoms at large momentum transfer. The eikonal wave impulse approximation and the semiclassical post-collision interaction model are used to analyse the momentum distortion in symmetric (e, 3−1e) reactions at intermediate energies. The effect of a strong interplay between electron–electron spatial correlation and momentum distortion is determined. The results of the analysis provide a guide for symmetric (e, 3−1e) experiments which are being carried out or are underway.

Due to recent progress in the studies of multiple ionization by electron impact [1] it has become possible to perform coincident double ionization experiments in the regime of large momentum transfer with good accuracy. In particular, the group in Rome has carried out a symmetric (e, 3−1e) experiment on the He atom[3]. To the best of our knowledge, this is the first such study of double ionization at large momentum transfer. In this experiment the energy of the projectile electron is 580 eV, the energies of the fast final electrons are 250 eV and the energy of the slow ejected electron is fixed by the energy conservation law at about 1 eV (see figure 1). The experimental kinematics has been chosen in accordance with the theoretical consideration [2], where it was argued that the symmetric (e, 3−1e) reactions in the regime of large momentum transfer allow the study of the effects of electron–electron correlations in the atomic wavefunction. There it was shown, in particular, that the radial correlation of electrons in the He atom yields the two-peak structure in the cross section. This is contrary to that predicted by the Hartree–Fock models, in which only a single peak is expected.

The predictions by Popov *et al* [2] are essentially based on the plane wave impulse approximation (PWIA) which is generally valid for symmetric binary electron–electron collisions at high electron energies and large momentum transfer [3, 4] (with respect to the

[3] Private communication by L Avaldi.

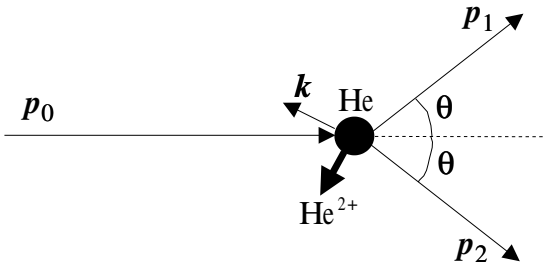

Figure 1. A schematic view of the symmetric (e, 3−1e) reaction in an He atom. The momenta p_0, p_1 and p_2 of the projectile and the fast final electrons, respectively, are in one plane. The two fast final electrons are detected in coincidence with equal energies ($E_1 = E_2 = E$) and equal angles relative to the projectile momentum ($\theta_1 = \theta_2 = \theta$). The energy of the slow ejected electron with momentum $\boldsymbol{k}$ is fixed by the energy conservation law. The cross section is studied as a function of θ.

average absolute values of one-electron energy and momentum in atom). Therefore, in the case of intermediate energies, their results must be revised by correcting the PWIA for the effects of distortion of the plane waves. It is generally known that the distortion originates from accounting for the interaction between the two electrons participating in the quasi-elastic impact collision and the rest of the system. In the present case, the interaction is of two types. The first is that of the initial and fast final electrons with the effective field in the intra-atomic domain, where the electron–electron impact collision takes place. The second is the post-collision interaction via the long-range Coulomb potential when the two fast final electrons and the rest of the system are at a large distance from each other.

In this letter we provide a general theoretical framework for the treatment of the effects of distortion in an electron-impact double-ionization experiment involving large momentum transfer. Within this framework we use the eikonal wave impulse approximation (EWIA) with the shell-averaged potential [5] and the semiclassical post-collision interaction (SCPCI) model [6] to analyse the momentum distortion in symmetric (e, 3−1e) reactions. Then, instead of the EWIA with the shell-averaged potential, we formulate the EWIA with the potential which is averaged in agreement with the model of one-electron orbitals in an atomic shell. Such an approach takes into account the dependence of the distortion's effects on the spatial correlation of the atomic electrons. The results of the numerical calculations show a strong interplay between the electron–electron space correlation and the momentum distortion. The consideration below is restricted to the He atom.

The energy and momentum conservation laws for the reaction depicted in figure 1 can be written as (atomic units (au) are used hereafter unless otherwise stated)

$$E_0 + \varepsilon^{\mathrm{He}} = 2E + E_k, \tag{1}$$

$$\boldsymbol{p}_0 = \boldsymbol{p}_1 + \boldsymbol{p}_2 + \boldsymbol{k} + \boldsymbol{q}, \tag{2}$$

where $\varepsilon^{\mathrm{He}} = -2.903$ au is the ground state energy of the He atom and $\boldsymbol{q}$ is the recoil momentum of the He^{2+} ion. The so-called four-fold differential cross section (4DCS) corresponding to the (e, 3−1e) reaction is given by

$$\frac{\mathrm{d}\sigma}{\mathrm{d}E_1\,\mathrm{d}E_2\,\mathrm{d}\Omega_1\,\mathrm{d}\Omega_2} = \frac{2p_1p_2k}{(2\pi)^8 p_0}\int \mathrm{d}\Omega_k |T(\boldsymbol{p}_1, \boldsymbol{p}_2, \boldsymbol{k}; \boldsymbol{p}_0, \Phi_0)|^2 \tag{3}$$

where $T(\boldsymbol{p}_1, \boldsymbol{p}_2, \boldsymbol{k}; \boldsymbol{p}_0, \Phi_0)$ is the four-body Coulomb amplitude and Φ_0 is the ground state wavefunction of the He atom. In what follows, we utilize in the evaluation of the amplitude a

perturbative method based on the frozen-core approximation. We divide the four-body system into two subsystems. One consists of the projectile and the atomic electrons which, after the quasi-elastic collision, become the fast electron pair, and the other consists of the He^{2+} ion and the slow ejected electron. In the frozen-core approximation, the second subsystem is supposed to be a spectator during the impact electron–electron collision in the first subsystem. Thus we derive for the amplitude

$$T(\boldsymbol{p}_1, \boldsymbol{p}_2, \boldsymbol{k}; \boldsymbol{p}_0, \Phi_0) = \int\int \frac{\mathrm{d}\boldsymbol{p}_1'}{(2\pi)^3}\frac{\mathrm{d}\boldsymbol{p}_2'}{(2\pi)^3}\frac{\mathrm{d}\boldsymbol{p}}{(2\pi)^3}\langle\Phi^-_{\boldsymbol{p}_1\boldsymbol{p}_2}|\boldsymbol{p}_1'\boldsymbol{p}_2'\rangle\langle\chi^-_{\boldsymbol{p}_1'}\chi^-_{\boldsymbol{p}_2'}|\hat{t}|\chi^+_{\boldsymbol{p}_0}\boldsymbol{p}\rangle\langle\boldsymbol{p}\varphi^-_{\boldsymbol{k}}|\Phi_0\rangle \quad (4)$$

where $\hat{t}$ is the binary ee-scattering operator, $\chi^{\pm}_{\boldsymbol{p}_i'}$ $(i = 0, 1, 2)$ are the distorted waves in the intra-atomic eikonal potential and $\varphi^-_{\boldsymbol{k}}$ is the outgoing Coulomb wave in the field of the He^{2+} ion. The function $\Phi^-_{\boldsymbol{p}_1\boldsymbol{p}_2}$ is a time-reversed scattering state of the three-body Hamiltonian with the total potential given by a sum of long-range parts of the Coulomb potentials between the electrons in the fast electron pair and between the fast electron pair and the second subsystem, respectively. Neglecting the long-range parts of the Coulomb potentials, the amplitude in the EWIA can be obtained from (4) as

$$T(\boldsymbol{p}_1, \boldsymbol{p}_2, \boldsymbol{k}; \boldsymbol{p}_0, \Phi_0) = \int \frac{\mathrm{d}\boldsymbol{p}}{(2\pi)^3}\langle\chi^-_{\boldsymbol{p}_1}\chi^-_{\boldsymbol{p}_2}|\hat{t}|\chi^+_{\boldsymbol{p}_0}\boldsymbol{p}\rangle\zeta(\boldsymbol{k}, \boldsymbol{p}) \quad (5)$$

with

$$\zeta(\boldsymbol{k}, \boldsymbol{p}) = \int\int \mathrm{d}\boldsymbol{r}_1\,\mathrm{d}\boldsymbol{r}_2\,\varphi^{-*}(\boldsymbol{k}, \boldsymbol{r}_1)\,\mathrm{e}^{-\mathrm{i}\boldsymbol{p}\boldsymbol{r}_2}\Phi_0(\boldsymbol{r}_1, \boldsymbol{r}_2). \quad (6)$$

Finally, neglecting in (5) the distorting eikonal potential, the PWIA can be expressed as

$$T(\boldsymbol{p}_1, \boldsymbol{p}_2, \boldsymbol{k}; \boldsymbol{p}_0, \Phi_0) = \langle\boldsymbol{p}_1\boldsymbol{p}_2|\hat{t}|\boldsymbol{p}_0\,\boldsymbol{p}\rangle\zeta(\boldsymbol{k}, \boldsymbol{p}), \quad (7)$$

with half-off-shell ee-scattering amplitude [7]

$$\langle\boldsymbol{p}_1\boldsymbol{p}_2|\hat{t}|\boldsymbol{p}_0\,\boldsymbol{p}\rangle = t\{\boldsymbol{p}_0 - \tfrac{1}{2}(\boldsymbol{p}_1 + \boldsymbol{p}_2), \tfrac{1}{2}(\boldsymbol{p}_1 - \boldsymbol{p}_2); [\tfrac{1}{2}(\boldsymbol{p}_1 - \boldsymbol{p}_2)]^2\} \quad (8)$$

where $\boldsymbol{p} = \boldsymbol{p}_1 + \boldsymbol{p}_2 - \boldsymbol{p}_0$.

From (6) it follows that in the PWIA (7) the 4DCS is proportional to the absolute square of the Fourier transform of the projection of the helium wavefunction Φ_0 onto the one-electron continuum Coulomb state $\varphi^-_{\boldsymbol{k}}$. This in principle allows for a direct investigation of the electron–electron correlations in the wavefunction of an He atom. In figure 2(a) the 4DCS (3) calculated in the PWIA with two different models for the helium wavefunction is shown. These wavefunctions are given by

$$\Phi_0(\boldsymbol{r}_1, \boldsymbol{r}_2) = \frac{1}{\sqrt{N}}(\mathrm{e}^{-ar_1-br_2} + \mathrm{e}^{-br_1-ar_2}) \quad (9)$$

with

$$N = 128\pi^2\left\{\frac{1}{(4ab)^3} + \frac{1}{(a+b)^6}\right\}. \quad (10)$$

The case $a = b$ corresponds to the wavefunction of Hylleraas [8] without correlations, and the case $a \neq b$ corresponds to the wavefunction of Hylleraas–Eckart–Chandrasehkar (HEC) [8–10] with radial correlation. It is clear from figure 2(a) that there is a qualitative difference between results using the Hylleraas and those using the HEC functions. The wavefunction of Hylleraas gives only a simple binary peak at about 40°, whereas the HEC wavefunction gives two peaks, the larger one at a smaller angle and the small peak at the larger angle. The two-peak structure in the case of the HEC wavefunction is explained by the interference of the amplitudes corresponding to the knock-out of an electron from different 1s orbitals.

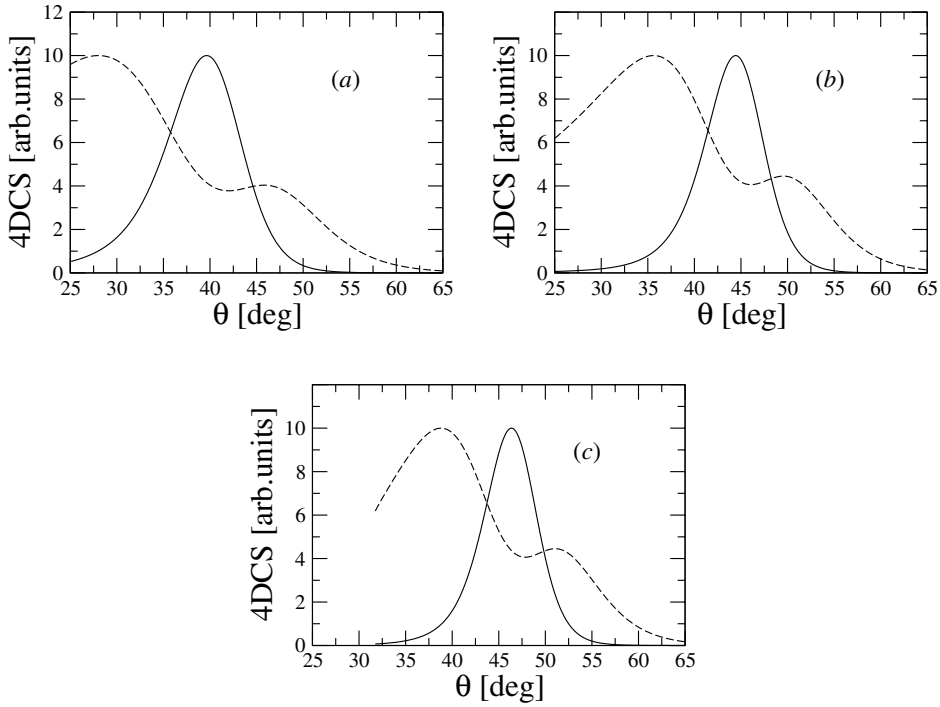

Figure 2. The 4DCS as a function of the angle θ between one of the fast electrons and the projectile electron (see figure 1). The projectile energy is $E_0 = 580$ eV and the energies of the fast and slow final electrons are $E = 250$ eV and $E_k = 1$ eV, respectively. The full curve is the wavefunction of Hylleraas and the broken curve is the HEC wavefunction. The results of the (*a*) PWIA, (*b*) EWIA and (*c*) EWIA along with the SCPCI model are shown. For the ease of comparison all results are normalized to one maximum and plotted in arbitrary units.

Now let us take into account the distortion of the plane waves in an effective intra-atomic field. For this purpose the EWIA (5) with shell-averaged potential [5] is used. This means we use the calculations in the PWIA (7), but with the following substitution of momenta $\boldsymbol{p}_i$ $(i = 0, 1, 2)$ in equations (8) and (6):

$$\boldsymbol{p}_i \to \hat{\boldsymbol{p}}_i \sqrt{p_i^2 - 2\bar{V}}. \tag{11}$$

The shell-averaged potential is assumed to be optical-like, $\bar{V} = \bar{V}_R + \mathrm{i}\bar{V}_I$, with the real part given by the virial theorem $\bar{V}_R = 2\varepsilon_0$, where ε_0 is the binding energy per electron in the atomic shell. In the case of an He atom, $\bar{V}_R = \varepsilon^{\mathrm{He}}$. The small imaginary part $\bar{V}_I$ is introduced in order to model the inelastic effects of the distortion. We use below a reasonable estimate $\bar{V}_I = 0.01\bar{V}_R$. The results presented in figure 2(*b*) indicate a significant shift of the 4DCS towards larger angles. The shift is stronger in the region of smaller angles, and therefore the PWIA results using the HEC function are more affected by the eikonal distortion than those using the Hylleraas function. Utilizing the SCPCI model [6] in order to describe the post-collision Coulomb distortion, the additional nonuniform shift of the EWIA results towards larger angles can be obtained (see figure 2(*c*)). The shift is given by the following estimate:

$$\Delta\theta = \frac{1}{8Er_0}\frac{\cos\theta}{\sin^2\theta}, \tag{12}$$

where r_0 is the radius of the one-electron orbital in an He atom. The estimate is valid if $\theta \gg \Delta\theta$.

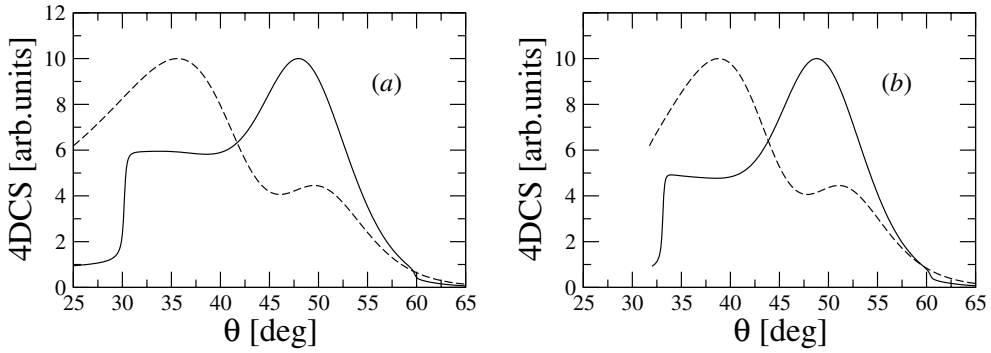

Figure 3. The 4DCS in the case of the HEC function using (*a*) the EWIA and (*b*) the EWIA along with the SCPCI model. The electron energies are the same as in figure 2. The case of the orbital-averaged potential is shown by the full curve and the broken curves correspond to those in figures 2(*b*) and (*c*), respectively. As in figure 2 all results are normalized to one maximum and plotted in arbitrary units.

Note that above we have neglected the spatial dependence of the distorting potential and have assumed that its real part is given by the virial theorem using a one-electron model of the atomic shell. Such an approach is justified if the wavefunction of Hylleraas is used, when both shell electrons are in identical 1s orbitals with $r_0 = a^{-1}$. However, in the case of the HEC wavefunction with radial correlation, the electrons occupy different 1s orbitals, with $r_0^a = a^{-1}$ and $r_0^b = b^{-1}$, respectively. The distorting potential is essentially different for different orbitals and we call it the orbital-averaged potential. In the EWIA (5) with orbital-averaged potential the 4DCS is

$$\frac{\mathrm{d}\sigma}{\mathrm{d}E_1\,\mathrm{d}E_2\,\mathrm{d}\Omega_1\,\mathrm{d}\Omega_2} = \frac{2p_1p_2k}{(2\pi)^8 p_0}\int \mathrm{d}\Omega_k\,|t^a\zeta^a + t^b\zeta^b|^2, \tag{13}$$

where $t^a(t^b)$ is given by (8) with substitution (11) for potential $\bar{V}^a$ ($\bar{V}^b$) and

$$\zeta^a = \frac{1}{\sqrt{N}}\int \mathrm{d}\boldsymbol{r}_1\,\varphi^{-*}(\boldsymbol{k},\boldsymbol{r}_1)\,\mathrm{e}^{-br_1}\int \mathrm{d}\boldsymbol{r}_2\,\mathrm{e}^{-\mathrm{i}\boldsymbol{p}^a\boldsymbol{r}_2}\,\mathrm{e}^{-ar_2}, \tag{14}$$

$$\zeta^b = \frac{1}{\sqrt{N}}\int \mathrm{d}\boldsymbol{r}_1\,\varphi^{-*}(\boldsymbol{k},\boldsymbol{r}_1)\,\mathrm{e}^{-ar_1}\int \mathrm{d}\boldsymbol{r}_2\,\mathrm{e}^{-\mathrm{i}\boldsymbol{p}^b\boldsymbol{r}_2}\,\mathrm{e}^{-br_2}. \tag{15}$$

The real part of the potential $\bar{V}^a(\bar{V}^b)$ is given by the virial theorem $\bar{V}_R^a = -a^2$ ($\bar{V}_R^b = -b^2$). It is seen that equation (13) reduces to the EWIA with shell-averaged potential if $a = b$.

In contrast to the EWIA with shell-averaged potential, equation (13) does not factorize. This leads to the nontrivial effect on the 4DCS which is shown in figure 3(*a*). Instead of the shift towards larger angles with respect to the PWIA calculations, a quite different two-peak structure is observed. As in the case of the PWIA and EWIA with shell-averaged potential, the two-peak structure is explained by the interference of the amplitudes corresponding to the knock-out of an electron from different 1s orbitals. However, now the momentum distortion depends on the orbital and thus, according to (13), strongly affects the interference. In the case of the orbital-averaged potential the use of the SCPCI model [6] must also be modified, because the radius of the one-electron orbital enters (12). According to (4) the modification implies that the amplitudes for different 1s orbitals in (13) are computed at different angles $\theta^a = \theta - \Delta\theta^a$ and $\theta^b = \theta - \Delta\theta^b$, respectively. As a result, 3(*b*) shows that, besides a shift towards larger angles with respect to the EWIA calculations, there is a change in the ratio between the two peaks. Thus, the effect of a strong interplay between the momentum distortion

and radial correlation can be clearly seen in figure 3. Significantly affecting the shape of the angular distribution, the effect can be observed experimentally on the arbitrary scale.

Several important remarks should be made regarding the results in figures 2 and 3. First, our calculations, which are not presented here, show that in the case of the shell-averaged potential the 4DCS is slightly sensitive to the imaginary part of the potential, whereas in the case of the orbital-averaged potential the imaginary part is important. In particular, increasing the imaginary part of the orbital-averaged potential we obtain the structure about 30°–35° (see figure 3) which is smoother and smaller in magnitude. This is connected with the behaviour of the ee-scattering amplitude (8) which, in the case of the orbital with a smaller radius in equation (13), becomes on-shell at $\theta \approx 30°$. Second, the wavefunction in the form (9) is simple and, for example, does not take into account the angular correlation. However, the results of the calculations using the shell-averaged potential and the more realistic wavefunctions with radial and angular correlations [11, 12] are very close to those in figure 2 for the HEC wavefunction. Therefore we believe that the results for the orbital-averaged potential in figure 3 provide at least a qualitative picture one would receive within equation (4) using the wavefunctions [11, 12]. Third, all the results have been presented on the arbitrary scale in order to illustrate the main effects of momentum distortion on the 4DCS, such as the shift and the change of shape with respect to the PWIA calculations. At the same time the momentum distortion also affects the magnitude of the 4DCS. Thus any future (e, 3−1e) measurements performed on the absolute scale can provide a deeper insight into the effects of momentum distortion and its interplay with electronic correlation.

In conclusion, we have investigated theoretically the effects of momentum distortion in symmetric (e, 3−1e) reactions at intermediate energies. The EWIA and the SCPCI models have been used in the analysis. Using the shell-averaged distorting potential with two parameters, the 4DCS can be moved towards larger angles. The shift is more pronounced at smaller angles, so the 4DCS becomes narrower than in the PWIA, but the overall shape for both the correlated and the uncorrelated wavefunctions is preserved. In contrast, using the orbital-average potential, we see the shift towards larger angles combined with the strong change of shape of the 4DCS in the case of a wavefunction with radial correlation. We expect the same effect if more realistic helium wavefunctions, which take into account both the radial and the angular correlations, are used. This investigation can serve as a guide for forthcoming symmetric (e, 3−1e) experiments at intermediate energies.

We are very grateful to Lorenzo Avaldi, Ochbadrakh Chuluunbaatar and Jamal Berakdar for useful discussions.

References

[1] Berakdar J and Kirschner J (ed) 2001 *Many-Particle Spectroscopy of Atoms, Molecules, Clusters and Surfaces* (New York: Plenum)
[2] Popov Yu V, Dal Cappello C and Kuzakov K 1996 *J. Phys. B: At. Mol. Opt. Phys.* **29** 5901
[3] Weigold E and McCarthy I E 1999 *Electron Momentum Spectroscopy* (New York: Kluwer)
[4] Neudatchin V G, Popov Yu V and Smirnov Yu F 1999 *Phys.–Usp.* **169** 1017
[5] Camilloni R, Giardini-Guidoni A, McCarthy I E and Stefani G 1980 *J. Phys. B: At. Mol. Phys.* **13** 397
[6] Avaldi L, Camilloni R, Popov Yu V and Stefani G 1986 *Phys. Rev.* A **33** 851
[7] Hostler L 1964 *J. Math. Phys.* **5** 591
[8] Hylleraas E A 1929 *Z. Phys.* **54** 347
[9] Eckart C 1930 *Phys. Rev.* **36** 878
[10] Chandrasekhar S 1944 *Astrophys. J.* **100** 176
[11] Bonham R A and Kohl D A 1966 *J. Chem. Phys.* **45** 2471
[12] Chuluunbaatar O, Puzynin I V and Vinitsky S I 2001 *J. Phys. B: At. Mol. Opt. Phys.* **34** L425